Journal of Applied Sciences

ISSN 1812-5654

science alert

ANSInet
an open access publisher
http://ansinet.com

OPEN ACCESS Journal of Applied Sciences

ISSN 1812-5654
DOI: 10.3923/jas.2025.1.10

Research Article
Leveraging MATLAB for Machine Learning-Based Identification of Alzheimer's Biomarkers Using PET Scan Data Analysis

[1]Irfan Biswas and [2]Md Helal Uddin Biswas

[1]Shrewsbury Sr. High School, 75 Cypress Ave, Shrewsbury, MA-01545, United States of America
[2]Adjunct Faculty, Massachusetts College of Pharmacy and Health Sciences University, Worcester, MA-01608, United States of America

Abstract

Background and Objective: Alzheimer's disease (AD) is characterized by the accumulation of beta-amyloid and Tau proteins in the brain, making early detection crucial for effective intervention. This study aims to develop a Matrix Laboratory (MATLAB)-based machine learning approach to enhance the identification of these biomarkers using positron emission tomography (PET) scan data, reducing the risk of misdiagnosis. **Materials and Methods:** Brain imaging data, specifically PET scans highlighting beta-amyloid and Tau protein accumulations, were processed using MATLAB. The images were transformed into 1D RGB data tables for analysis. Machine learning models, including Fine K-Nearest Neighbors (KNN), Support Vector Machines (SVM) and neural networks, were trained and validated using MATLAB's Classification Learner App to classify different severity levels of protein accumulation. The study involved a total of 5,402 PET scan images, split into training and testing datasets. **Results:** The MATLAB-based analysis demonstrated a high level of accuracy in identifying protein accumulation levels, achieving a test accuracy of 97.6% with the Fine KNN model and 98.07% with neural networks on new, unseen data. The RGB analysis technique effectively differentiated between healthy, medium-unhealthy and unhealthy biomarker levels, providing a reliable tool for evaluating AD progression. The automated approach significantly reduced the potential for human error in interpreting PET scan images. **Conclusion:** The study showcases the potential of using MATLAB for automated analysis of PET scans in diagnosing Alzheimer's disease. This approach provides an efficient and accurate method for early detection, offering valuable insights for medical professionals and contributing to advancements in AD diagnostics.

Key words: Alzheimer's disease (AD), MATLAB, K-Nearest Neighbors (KNN) algorithm, machine learning, Tau protein

Citation: Biswas, I. and M.H. Biswas, 2025. Leveraging MATLAB for machine learning-based identification of Alzheimer's biomarkers using PET scan data analysis. J. Appl. Sci., 25: 1-10.

Corresponding Author: Md Helal Uddin Biswas, Adjunct Faculty, Massachusetts College of Pharmacy and Health Sciences University, Worcester, MA-01608, United States of America

Competing Interest: The authors have declared that no competing interest exists.

Data Availability: All relevant data are within the paper and its supporting information files.

INTRODUCTION

The AD is a neurodegenerative progressive illness affecting millions worldwide[1], characterized by cognitive decline, memory loss and behavioral changes. Underlying pathologies of AD include the deposition of beta-amyloid plaques and Tau protein tangles in the brain[2], which further leads to neuronal dysfunction and death. The early detection of these biomarkers[3-6] will enable timely intervention, slowing the progression of the disease and offering patients access to clinical trials and treatments targeting the early stages of AD.

Because it is an imaging modality based on the use of radiotracers, positron emission tomography (PET) can demonstrate metabolic activity in the brain and, therefore, provides extensive views for detecting abnormal metabolic processes associated with the disease. Using a PET scan, it is possible to detect beta-amyloid and Tau accumulation[7] before significant structural changes can be observed using computed tomography or magnetic resonance imaging. The PET scans are also able to show both typical and atypical metabolic activity and detect the atypical metabolism of tracers even before the disease shows up on other image processing techniques, such as Computerized Tomography (CT) and Magnetic Resonance Imaging (MRI)[8-12]. However, the interpretation of PET usually presents a challenge and as many as 20% of AD cases could be misdiagnosed[8,13,14], due to the semi-quantitative nature of the visual check and workload from professional medical grading. These challenges range from the subjective nature of interpretation to quantitative measures that can improve the diagnostic accuracy of PET scans.

The standard method of analyzing PET imaging depends to a great extent on subjective visual assessments, which may not detect subtle changes by the human eye and the extent of pathological involvement may be misinterpreted. Advanced image processing applications were thus introduced to transform these PET scans into quantitative data from simple DICOM, Digital Imaging and Communications in Medicine Formatted images[15,16], format images for further analysis. In that respect, it would be possible to transform visible information into numerical data by extracting RGB values from images. Color intensity corresponds to the level of the tracer uptake and hence, the extent of biomarker accumulation.

Machine learning has now emerged as a promising tool to automate classification and analysis tasks in medical image processing, serving to find patterns and correlations that are not obvious through other techniques. This research study will examine the efficacy in the improvement of detection and classification of AD severity by applying ML techniques in concert with RGB image zoning to PET scan data. Automation in PET image analysis, as proposed in this study, serves as a more objective, reliable and accurate modality for identifying early stages of Alzheimer's disease that could considerably improve diagnostic precision and patient outcomes.

MATERIALS AND METHODS

Study area: This study was conducted from MATLAB[17] at home and at Shrewsbury High School Computer Lab, coursed June, 2022 to May, 2024.

Methodology: A series of methods were used to help construct this project and collect the data necessary to process through a pre-trained ML algorithm. One of the primary steps needed to obtain data was through data collection across various datasets[18], samples and possible research and images available online of PET scans of beta-amyloid and Tau proteins (Fig. 1a-f). There was a total of 5,402 images[17], where each was subdivided into three subfolders: 'healthy', 'medium-unhealthy' and 'unhealthy'. The images were processed using MATLAB's Image Segmenter App to isolate Regions of Interest (ROIs)[19,20] in the PET scans. Segmenting is an important preprocessing technique to reduce unnecessary or reduced information, or noise, from affecting the accuracy of subsequent analysis. Thresholding was a segmenting technique used to threshold specific RGB values. This thresholding technique was used to create the response variable, as seen in Fig. 2, for the neural network (NN) model and classify RGB values into a total of three classes. More specifically, Fig. 2a created multiple classes of intensities to create the response variable. For example, Fig. 2b showcased a variable spectrum: A color-based variable spectrum of infrared, red, orange, yellow, green, cyan, blue, violet and ultraviolet with wavelengths from 700 to 400 nm were all used to set different thresholds for each RGB color.

Multiple "labels" were used to signify an RGB color below 120, between 120 and 200 and above 200 RGB values. More specifically, a color designation of blue or green would be labeled as 'healthy', yellow and orange as 'medium-unhealthy' and a color of red being severely 'unhealthy'. 'Medium-unhealthy' was classed by RGB values between 120 and 200 and 'unhealthy' was classed by RGB values greater than 200. After segmenting images, they were combined using the combine function in MATLAB and combined with a total of 5,402 images to be processed by pre-trained ML algorithms. This procedure of segmenting and organizing the 2D images into a 1D format was repeated until

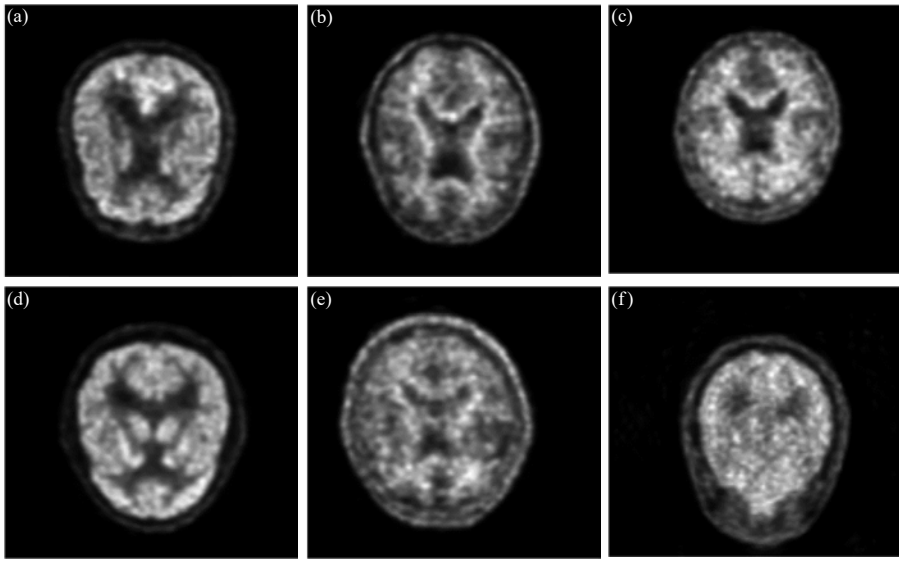

Fig. 1(a-f): PET scan of Tau protein Images, (a-f) PET scan Images
Source: ADNI

(a)

```
data = readtable('Data 3.xlsx');

% Initialize an empty cell array for 'color_intensity'
color_intensity = cell(height(data), 1);

for i = 1:height(data)
    if any(data{i, 1:630} > 200)
        color_intensity{i} = 'light';
    elseif any((data{i, 1:630} > 110) & (data{i, 1:630} <= 200))
        color_intensity{i} = 'medium';
    else
        color_intensity{i} = 'not light';
    end
end

% Convert 'color_intensity' to a categorical array
color_intensity = categorical(color_intensity);

% Add 'color_intensity' to 'data' as a new variable
data.color_intensity = color_intensity;
```

(b)

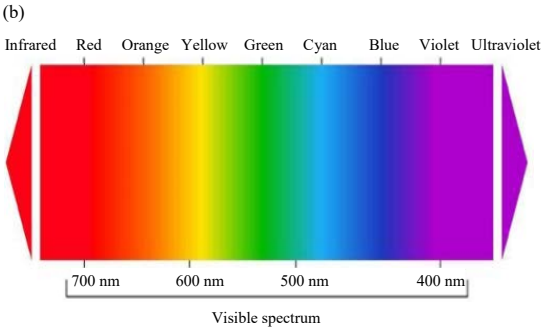

Fig. 2(a-b): Creating the response variable, (a) Multiple classes of intensities were created to create the response variable and (b)Variable spectrum: Color-based variable spectrum of infrared, red, orange, yellow, green, cyan, blue, violet and ultraviolet with wavelength from 700-400 nm

all images were able to be processed into a combined data table. The thresholding method also allows for the removal of any unwanted attributes, missing values and redundant records by analyzing the frequency of the RGB colors. Additionally, splitting the data was required for creating both test and training data. The model was trained from training set data and then tested upon newly unseen data to help counter the possibility of overfitting or the ability of the algorithm to simply memorize the training data. This was done by splitting 22% of the training data into testing data. Furthermore, Bayesian Optimization[21] was instrumental in improving model performance by efficiently selecting hyperparameters. Unlike traditional methods such as grid search or random search, Bayesian Optimization uses probabilistic models to prioritize hyperparameters with the highest potential to improve accuracy. This approach likely contributed to the Fine KNN model achieving its superior test accuracy of 98.07%, as it allowed the optimization process to focus on the most impactful parameter combinations. The performance of the ML models was assessed using standard evaluation metrics, including accuracy, precision, recall and F1 scores. These metrics were calculated from the confusion matrices

generated for each model. The formulas[18] used to calculate these metrics were as follows:

$$\text{Precision} = \frac{T_p}{T_p + F_p}$$

where, T_p represents true positives and F_p false positives. Precision quantifies the proportion of correctly predicted positive observations:

$$\text{Recall} = \frac{T_p}{T_p + T_n}$$

where, T_n represents true negatives. Recall measures the proportion of actual positives that were correctly identified:

$$F_1 \text{ score} = \frac{2(\text{Precision} \times \text{Recall})}{\text{Precision} + \text{Recall}}$$

which provides a harmonic mean of precision and recall to balance false positives and false negatives.

These formulas were instrumental in evaluating model performance across the three classes ('healthy', 'medium-unhealthy' and 'unhealthy') and ensuring the consistency of results.

RESULTS

This study utilized MATLAB and its suite of tools to analyze PET scan data and develop machine learning (ML) models for classifying Alzheimer's disease (AD) biomarkers. A total of 5,402 PET scan images were collected from the Alzheimer's Disease Neuroimaging Initiative (ADNI) database. The workflow, summarized in Fig. 3, involved segmenting and augmenting these images, preprocessing them into datasets and training ML algorithms to classify images into three categories: Healthy individuals, individuals with AD and individuals exhibiting various levels of disease progression.

The preprocessing phase included segmentation techniques to isolate Regions of Interest (ROIs), thresholding to assign RGB values and augmentation to prepare images for efficient analysis. Image segmentation reduced noise and ensured accurate data extraction by isolating meaningful regions in the scans. Thresholding was applied to classify image regions based on RGB values: Blue and green pixels (RGB values <120) were categorized as healthy, yellow and orange pixels (RGB values 120-200) were classified as medium-unhealthy and red pixels (RGB values >200) were labeled as unhealthy. The performance of various machine learning models was evaluated based on their test accuracy and computational cost during training, as shown in Fig. 4. Figure 4a presents the test accuracy of Decision Trees (TREE), Neural Networks, Support Vector Machines (SVMs) and K-Nearest Neighbors (KNN). Among these models, the neural network achieved the highest test accuracy at 98.07%, followed by SVM at 96.98%, KNN at 96.74% and TREE at 96.62%.

In addition to test accuracy, the total computational cost required for training these models was compared, as shown in Fig. 4b. The TREE model incurred the highest computational cost 28, while Neural Networks had a cost of 16, SVMs 25 and KNN 27. These results demonstrate a trade-off between computational efficiency and classification performance. Neural Networks and SVMs consistently achieved higher accuracy rates while maintaining moderate computational costs. TREE models, despite requiring fewer computational resources, exhibited slightly lower accuracy. The KNN models showed a balance between accuracy and computational cost.

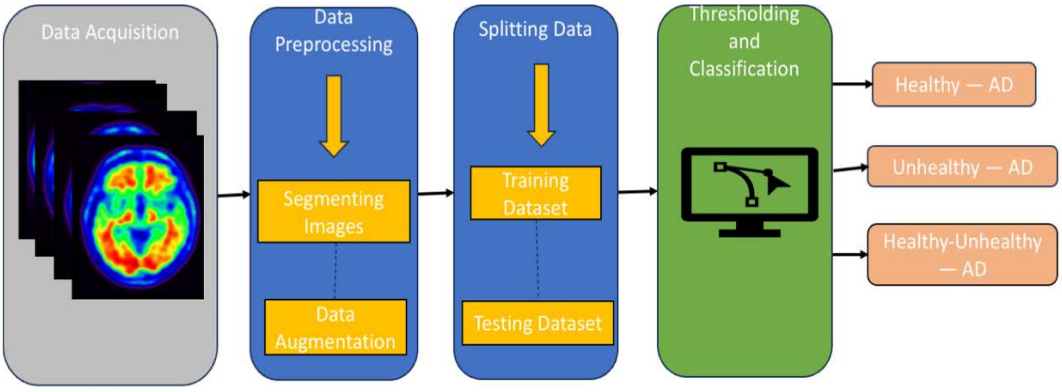

Fig. 3: Workflow research algorithm

First of all, acquisition of data, then processing of data by segmentation of images and data augmentation, then splitting of data with training dataset and testing dataset. Followed by thresholding and classification as healthy individuals and unhealthy individuals with AD. Alzheimer's disease and healthy-unhealthy with AD

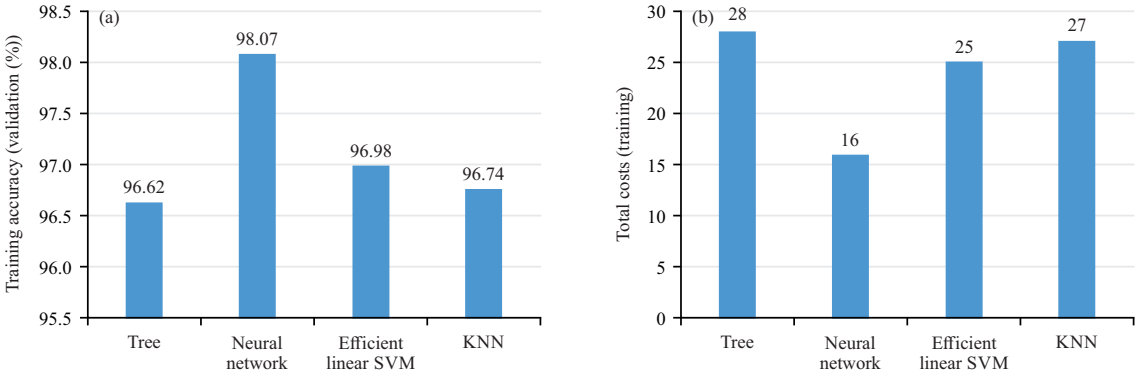

Fig. 4(a-b): Training data of test accuracy (validation) and test cost (training), (a) Test Accuracy and (b) Test cost

(a) Test accuracy with TREE, 96.62%, Neural network, 98.07%; Effective learning SVM, 96.98% and KNN, 96.74% and (b) Total cost data with TREE, 28; Neural network, 16, Effective learning SVM, 25 and KNN, 27. Support Vector Machines (SVMs) and K-Nearest Neighbors (KNN)

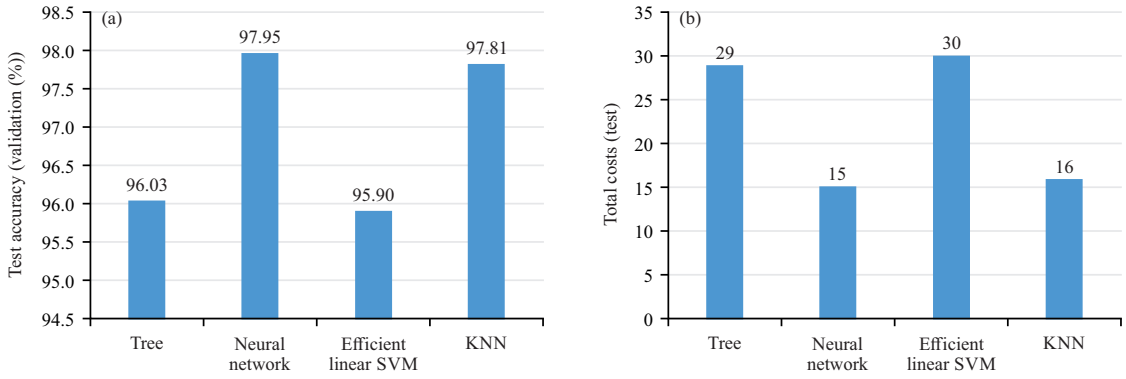

Fig. 5(a-b): Test data of test accuracy (validation) and test cost (tests), (a) Test Accuracy and (b) Total cost

(a) Test accuracy with TREE, 96.03%; Neural network, 97.95%; Effective learning SVM, 95.90% and KNN 97.81% and (b) Total cost data with TREE, 29; Neural network, 15; Effective learning SVM, 30 and KNN, 16. Support Vector Machines (SVMs) and K-Nearest Neighbors (KNN)

Once trained, the models were tested on a separate dataset to evaluate their generalization performance. The test accuracy for each machine learning model is summarized in Fig. 5a. Among the models, the Fine KNN model demonstrated high test accuracy at 97.81%, closely followed by Neural Networks at 97.95%. The Decision Trees (TREE) model achieved a test accuracy of 96.03%, while Support Vector Machines (SVMs) achieved 95.90%. The corresponding computational costs for testing these models are presented in Fig. 5b. Neural networks were the most computationally efficient with a cost of 15, followed by KNN at 16. Decision Trees required a computational cost of 29, while SVMs required the highest cost at 30. These results illustrate the trade-offs between model accuracy and computational efficiency during the testing phase.

The confusion matrix for the Medium Neural Network model, displayed in Fig. 6a, provides detailed counts for true positives, false positives, true negatives and false negatives across all three categories: Healthy, medium-unhealthy and unhealthy. For example, the matrix shows that the true positive rate for the healthy category was 99.1%, while the medium-unhealthy category exhibited a precision of 81.6% and a recall of 86.96%. These discrepancies are further highlighted in Fig. 6a, which illustrates the distribution of classification results. The medium-unhealthy class had the highest proportion of false positives, with 0.8% of samples being misclassified as unhealthy, compared to 0.9% for the healthy class and 0.8% for the unhealthy class. Additionally, the medium-unhealthy category showed a false negative rate of 13.4%, indicating that a significant proportion of actual medium-unhealthy samples were incorrectly classified as either healthy or unhealthy. These results demonstrate that while the model performed well overall, the intermediate medium-unhealthy category posed the greatest challenge, likely due to its overlap with the healthy and unhealthy categories.

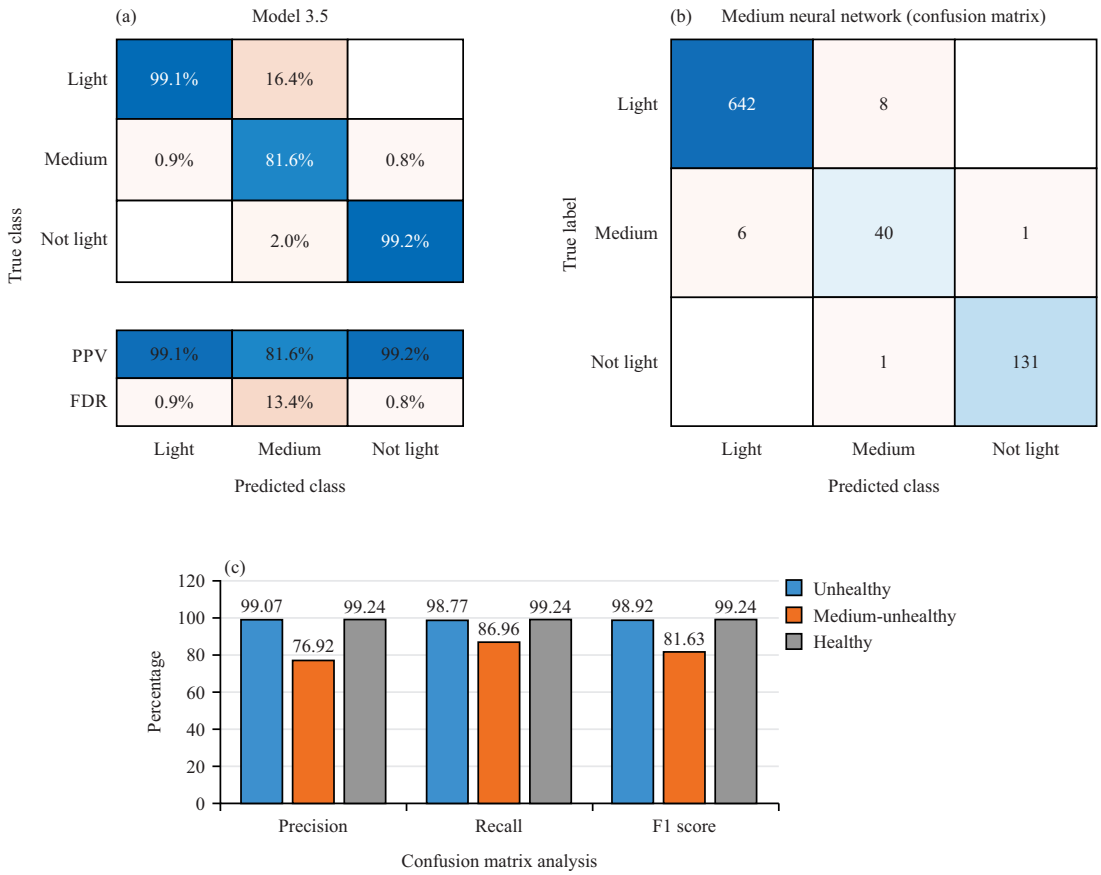

Fig. 6(a-c): Confusion matrix for the medium neural network, (a) Comparison of observations made for false positives, (b) Total observations made regarding the medium neural network and (c) Confusion matrix analysis of precision, recall and F1 score

The classification performance of the model was evaluated using precision, recall and F1 scores for the three classes: Light (healthy), medium (medium-unhealthy) and not light (unhealthy), as illustrated in Fig. 6c. The model demonstrated excellent performance for the light and not light classes. For the light class, the precision was 99.07%, the recall was 98.77% and the F1 score was 98.92%. Similarly, for the not light class, precision, recall and F1 scores were all 99.24%, indicating highly reliable classification for these categories.

In contrast, the performance for the medium class was comparatively lower. The precision for this class was 76.92%, the recall was 86.96% and the F1 score was 81.63%. These metrics indicate that the model was less effective in accurately identifying medium instances compared to light and not light categories, likely due to overlapping features or ambiguities between classes. Despite this, the overall results confirm the robustness of the model in distinguishing the majority of instances across the three classes.

The receiver operating characteristic (ROC) curve analysis, shown in Fig. 7a, further validated the model's classification performance. The curve shows the trade-off between true positive rates and false positive rates across all thresholds. The area under the curve (AUC) was 0.971, indicating excellent classification performance. Figure 7a illustrates the true positive rates (TPR) for each category, with the healthy class achieving the highest TPR at 97.2%, followed by the unhealthy class at 99.93%. However, the medium-unhealthy class exhibited a slightly lower TPR of 89.91%, reflecting the model's difficulty in correctly classifying intermediate cases. This discrepancy highlights a potential need for additional training data or further refinement of the model for this category. Figure 7b exemplifies lower classfiication errors and improvements of the model. Overall, the lower minimum classfication error after multiple iterations displays the ability of classifying new batches of data and scans with higher accuracy. Additionally, Fig. 7c demonstrates the impact of optimization techniques on overall classification performance.

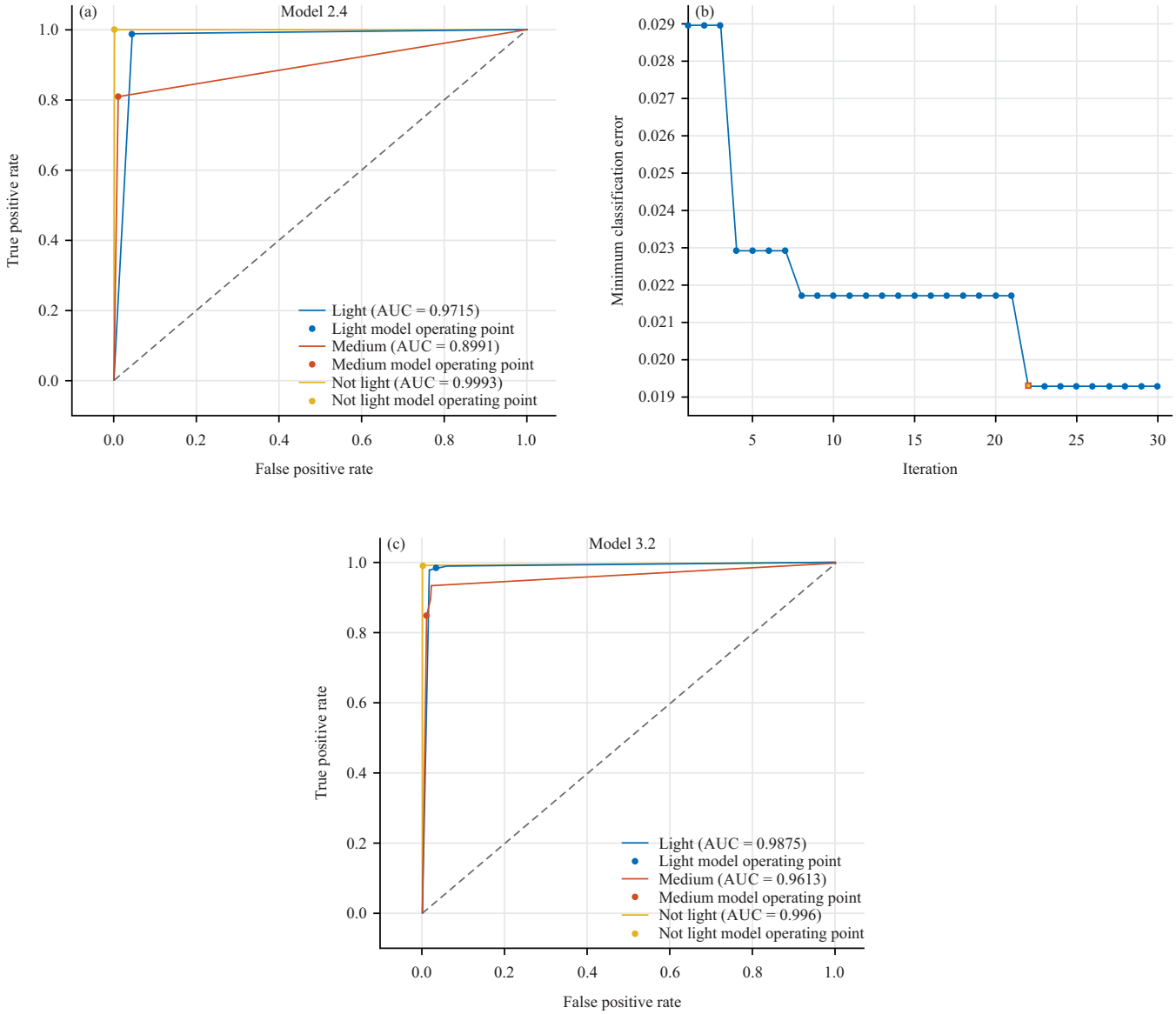

Fig. 7(a-c): Minimum classification plot and ROC curve validation, (a and c) ROC curve validation which makes the accuracy, or validation, of the specified model and the ability for the model to classify the data, represents a fine KNN model that is being compared against evidently and lacks the classification accuracy of (a) in classifying a 'medium' RGB. (b) Minimum classification plot of the optimized neural network. The plot is a result of changing optimization techniques and fine-tuning

After fine-tuning the model using Bayesian Optimization, the medium neural network achieved an area under the curve (AUC) score of 0.987 and an accuracy improvement of 2.5% compared to the unoptimized version. The optimization process focused on key hyperparameters, such as learning rate and number of layers, enabling the model to achieve robust performance while maintaining computational efficiency.

In summary, MATLAB's segmentation, thresholding and augmentation tools, combined with advanced ML algorithms, enabled the precise classification of AD biomarkers in PET scan images. The Fine KNN model achieved the highest accuracy, while Bayesian Optimization and ROC curve analysis highlighted the robustness of the Medium Neural Network model. Figure 4-7 collectively demonstrate the balance between accuracy, computational cost and optimization across various models, underscoring the potential of ML-based approaches for analyzing AD biomarkers and improving diagnostic methodologies.

DISCUSSION

In the first batch of 200 images, the training and testing data were as follows. Figure 4a, displayed test accuracy with TREE, 96.62%; neural network, 98.07%; effective learning SVM, 96.98% and KNN, 96.74%. Overall, as shown in Fig. 4b, the total cost of data with TREE was 28; neural network, 16; effective learning SVM, 25 and KNN, 27. The approach taken in this study is novel, using MATLAB-based machine learning as a means of analyzing PET for the detection and classification of beta-amyloid and Tau protein accumulations seen in AD. During the second batch of 350 images, in Fig. 5a-b, the test accuracy with this approach was effective with new data, at 97.81% using the Fine KNN model and 97.95% using neural networks, thus distinguishing very well between states of health, medium-unhealthy and unhealthy biomarker accumulation levels. These findings demonstrate the power of this method in the automation of complicated imaging analyses and in reducing human errors for earlier and more accurate diagnosis of AD.

The findings align with and build upon previous work in the field. Among these is the work of Barragán-Montero *et al.*[10], regarding the use of AI to improve such diagnostic performance at the level of medical imaging, identifying machine learning as one of the strategic technologies that work for the reduction of errors in manual analysis. Indeed, the present study confirms these observations and extends them with an application of machine learning in the field of PET scan analysis for Alzheimer's biomarkers, representing a practical solution to the big clinical challenge. Similarly, Bao *et al.*[13] highlighted how valuable it is for radiotracers to map out changes in AD with PET imaging and hence proved that this decision to use PET as a base modality was not wrong. Combining this imaging with modern machine learning brings a large step in this work toward leveraging PET scan data for early-stage diagnosis.

These findings are also in agreement with those of Zukotynski *et al.*[14] who, while explaining the value of PET/CT for dementia diagnosis, underlined that combining imaging modalities will be important for enhancing the sensitivity of diagnoses. In this respect, the strategy of the present study is, approaching the analysis of PET data in a very accurate way through MATLAB-can represent a complementary method to such diagnostic techniques. Prasath and Sumathi[9] indicated "there is a dire need for early detection techniques in AD for arresting the disease progress and its management". This objective directly becomes the aim of this study by implementing correct machine learning models. In turn, Reiman and Jagust[6] described weaknesses in manual analysis within the framework of early diagnosis of AD due to a failure to usually observe subtle changes in analyzed scanned PET images because of human fatigue and error. The automation of the process of image analysis, as this method does, overcomes such limitations and provides proof that machine learning may greatly enhance this process of detection. Similarly, an article by Therriault *et al.*[12] also indicated the usefulness of Tau PET imaging for the understanding and progression of AD. This study's emphasis on both imaging features of Tau and beta-amyloid imaging promotes this understanding in the development of a comprehensive method to evaluate different biomarkers. Secondly, in agreement with Cheng *et al.*[5] who focused their work on the predictive capability of plasma biomarkers, are further supported by Therriault *et al.*[12] which complements this work with imaging-based biomarkers. In that respect, these approaches can be integrated to establish a more holistic diagnostic framework, which considers both blood-based and imaging biomarkers.

The implications brought about by this study are significant as it focuses on a MATLAB-based framework for automating the analysis of PET scans, hence addressing one of the big bottlenecks in the diagnostics of AD, which is manual interpretation. This would enhance the coherence of diagnosis and provide a standardized means that is susceptible to less subjective bias which may lead to better patient outcomes. Furthermore, the fact that this study was able to achieve such high accuracy using a relatively small data set speaks to the robustness of the model. It also underlines the need for further validation with larger sample sizes. That is because a limitation is dependency on high-quality imaging data since model performances can be different depending on the variable image resolution and image quality. However, this constitutes a common challenge in imaging research, which can be mitigated through standardized imaging protocols.

This MATLAB-based methodology can easily be extended to the study of other neurodegenerative disorders such as Parkinson's disease or multiple sclerosis, where similar imaging problems are observed. This could be extended to diagnose other biomarkers or the use of various imaging techniques, such as MRI. It could be further fine-tuned with deep learning techniques, such as CNN, which would give more subtle pattern recognition with higher accuracy.

It has been pointed out by Wang *et al.*[3] that as PET and MRI may complement each other in imaging AD's pathophysiology, this might be a direction for the future of this study. Future studies should be conducted to enhance the size of the dataset by diversifying the PET scans to ensure the generality of the models across multiple demographic groups and at different stages of the disease. Such would also tend to

mitigate against the possibility of overfitting and improve predictive performance in more realistic scenarios. There could also be a collaboration with clinical research institutions to ensure that trials using real-world data are conducted to verify the utility of the technique in practical, everyday clinical applications, enabling translation into every day diagnostics far more quickly than might otherwise be possible with automated analysis. Advancements like these could mean a sea change in the diagnosis and treatment of Alzheimer's disease, offering for the first time a clear route to more effective interventions and improved patient care.

CONCLUSION

The present study illustrates that the proposed machine learning algorithm could determine biomarkers for Alzheimer's disease, including beta-amyloid and Tau proteins, from PET scan data interpretation with much higher accuracy and speed. This automated technique eliminates the possibility of errors caused by human intervention and represents a very useful diagnostic aid for early diagnosis, which is highly important for the effective treatment and management of Alzheimer's disease. Future studies should be directed at the validation of this approach on larger datasets and its extension to other neurodegenerative disorders. The inclusion of other imaging modalities like MRI will further enhance the diagnostic capability and provide a more integrated framework for clinical use.

SIGNIFICANCE STATEMENT

The study enhances early detection of Alzheimer's disease through MATLAB-based machine learning techniques, analyzing PET scan data to identify key biomarkers like beta-amyloid and Tau proteins. This approach offers a more accurate and automated analysis of brain images, reducing the risk of misdiagnosis and enabling timely intervention. The results demonstrate that this machine learning algorithm can accurately classify protein accumulation with a 97.6% test accuracy, showcasing its potential as a reliable tool for diagnosing Alzheimer's disease and contributing to the development of advanced diagnostic methods.

REFERENCES

1. Bondi, M.W., E.C. Edmonds and D.P. Salmon, 2017. Alzheimer's disease: Past, present, and future. J. Int. Neuropsychological Soc., 23: 818-831.
2. Armstrong, R.A., 2013. What causes Alzheimer's disease? Folia Neuropathol., 51: 169-188.
3. Wang, J., C. Jin, J. Zhou, R. Zhou, M. Tian, H.J. Lee and H. Zhang, 2023. PET molecular imaging for pathophysiological visualization in Alzheimer's disease. Eur. J. Nucl. Med. Mol. Imaging, 50: 765-783.
4. Bloom, G.S., 2014. Amyloid-β and tau: The trigger and bullet in Alzheimer disease pathogenesis. JAMA Neurol., 71: 505-508.
5. Cheng, L., W. Li, Y. Chen, Y. Lin, B. Wang, Q. Guo and Y. Miao, 2022. Plasma Aβ as a biomarker for predicting Aβ-PET status in Alzheimer's disease: A systematic review with meta-analysis. J. Neurol. Neurosurg. Psychiatry, 93: 513-520.
6. Reiman, E.M. and W.J. Jagust, 2012. Brain imaging in the study of Alzheimer's disease. NeuroImage, 61: 505-516.
7. Perovnik, M., A. Vo, N. Nguyen, J. Jamšek and T. Rus *et al*., 2022. Automated differential diagnosis of dementia syndromes using FDG PET and machine learning. Front. Aging Neurosci., Vol. 14. 10.3389/fnagi.2022.1005731.
8. Nichols, J.A., H.W.H. Chan and M.A.B. Baker, 2019. Machine learning: Applications of artificial intelligence to imaging and diagnosis. Biophys. Rev., 11: 111-118.
9. Prasath, T. and V. Sumathi, 2023. Identification of Alzheimer's disease by imaging: A comprehensive review. Int. J. Environ. Res. Public Health, Vol. 20. 10.3390/ijerph20021273.
10. Barragán-Montero, A., U. Javaid, G. Valdés, D. Nguyen and P. Desbordes *et al*., 2021. Artificial intelligence and machine learning for medical imaging: A technology review. Physica Med., 83: 242-256.
11. Sharma, G., 2017. Performance analysis of image processing algorithms using MATLAB for biomedical applications. Int. J. Eng. Manuf., 7: 8-19.
12. Therriault, J., M. Vermeiren, S. Servaes, C. Tissot and N.J. Ashton *et al*., 2023. Association of phosphorylated tau biomarkers with amyloid positron emission tomography vs tau positron emission tomography. JAMA Neurol., 80: 188-199.
13. Bao, W., F. Xie, C. Zuo, Y. Guan and Y.H. Huang, 2021. PET neuroimaging of Alzheimer's disease: Radiotracers and their utility in clinical research. Front. Aging Neurosci., Vol. 13. 10.3389/fnagi.2021.624330
14. Zukotynski, K., P.H. Kuo, D. Mikulis, P. Rosa-Neto, A.P. Strafella, R.M. Subramaniam and S.E. Black, 2018. PET/CT of dementia. Am. J. Roentgenol., 211: 246-259.
15. Teh, V., K.S. Sim and E.K. Wong, 2016. Brain early infarct detection using gamma correction extreme-level eliminating with weighting distribution. Scanning, 38: 842-856.
16. Petersen, R.C., P.S. Aisen, L.A. Beckett, M.C. Donohue and A.C. Gamst *et al*., 2010. Alzheimer's Disease Neuroimaging Initiative (ADNI): Clinical characterization. Neurology, 74: 201-209.
17. Markiewicz, T., 2011. Using MATLAB software with Tomcat server and Java platform for remote image analysis in pathology. Diagn. Pathol., Vol. 6. 10.1186/1746-1596-6-S1-S18.

18. García, S., S. Ramírez-Gallego, J. Luengo, J.M. Benítez and F. Herrera, 2016. Big data preprocessing: Methods and prospects. Big Data Anal., Vol. 1. 10.1186/s41044-016-0014-0.
19. Katako, A., P. Shelton, A.L. Goertzen, D. Levin and B. Bybel *et al*., 2018. Machine learning identified an Alzheimer's disease-related FDG-PET pattern which is also expressed in Lewy body dementia and Parkinson's disease dementia. Sci. Rep., Vol. 8. 10.1038/s41598-018-31653-6.
20. Chowdhury, M.A.Z., K. Ok, Y. Luo, Z. Liu and S. Chen *et al*., 2022. *ROI-Finder*: Machine learning to guide region-of-interest scanning for X-ray fluorescence microscopy. J. Synchrotron Radiat., 29: 1495-1503.
21. Elshewey, A.M., M.Y. Shams, N. El-Rashidy, A.M. Elhady, S.M. Shohieb and Z. Tarek, 2023. Bayesian optimization with support vector machine model for Parkinson disease classification. Sensors, Vol. 23. 10.3390/s23042085.